The dynamics and mixing of turbulent plumes in a turbulently convecting environment

FRED WITHAM AND JEREMY C. PHILLIPS

Department of Earth Sciences, University of Bristol, Queen's Road, Bristol, BS8 1RJ, UK

The turbulent motion of buoyant plumes released into turbulently convecting environments is studied. By assuming that the turbulent environment removes fluid from the plume at a rate proportional to a characteristic environmental velocity scale, we derive a model describing the fluid behaviour. For the example of pure buoyancy plumes, entrainment dominates near the source and the plume radius increases with distance, while further from the source removal, or *extrainment*, of plume material dominates, and the plume radius decreases to zero. Theoretical predictions are consistent with laboratory experiments, a major feature of which is the natural variability of the convection. We extend the study to include the evolution of a finite confined environment, the end-member regimes of which are a well-mixed environment at all times (high convective velocities), and a 'filling-box' model similar to that of Baines & Turner (1969) (low convective velocities). These regimes, and the motion of the interface in a 'filling-box' experiment, match experimental observations. We find that the convecting filling box is not stable indefinitely, but that the density stratification will eventually be overcome by thermal convection. The model presented here has important applications in volcanology, ventilation studies and environmental science.

1. Introduction

The behaviour of turbulent plumes (sustained releases of buoyant fluid) in uniform and stratified environments was first described by Morton, Taylor & Turner (1956). A characteristic of turbulent flows, such as jets, plumes or wakes, is the incorporation of surrounding fluid into the flow, or *entrainment* (List 1982; Rajaratnam 1976). Morton *et al.* (1956) argued, on dimensional grounds, that the plume radius must scale with distance from the source, and identified that this required the entrainment velocity, u_{in}, to be proportional to the vertical velocity within the plume, w. After Morton *et al.* (1956), the *entrainment constant*, α, can be defined by

$$u_{in} = \alpha w, \qquad (1.1)$$

with an experimentally determined value of 0.1 (Lee & Chu 2003). Subsequent experiments have shown this description to be in excellent agreement with laboratory experiments and field observations over five orders of magnitude (Turner, 1979, p. 199). By conserving mass, momentum and buoyancy through control volumes and using the Boussinesq approximation (the assumption that density differences are negligible except in buoyancy terms), Morton *et al.* (1956) derived three coupled ordinary

differential equations that describe the behaviour of the plume:

$$\frac{d(b^2 w)}{dz} = 2b\alpha w, \tag{1.2}$$

$$\frac{d(b^2 w^2)}{dz} = b^2 g', \tag{1.3}$$

$$\frac{d(b^2 w g')}{dz} = -b^2 w N(z)^2, \tag{1.4}$$

where b is the plume radius, z is the vertical distance from the plume origin, g' is the reduced gravity defined by

$$g' = g \left(\frac{\rho - \rho_a}{\rho_a} \right) \tag{1.5}$$

and $N(z)$ is the buoyancy frequency or Brunt–Väisälä frequency defined by

$$N(z)^2 = \frac{g}{\rho_a} \frac{d\rho_a}{dz}. \tag{1.6}$$

Here ρ is the plume density, ρ_a is the density of the environment at a given height and g is the gravitational acceleration. Note that in the infinite environment case ρ_a is equal to the density of the environment at the source height, but this is not valid in the general case (§4).

This work extends the description of plumes to include those in a turbulently convecting environment. This has applications in volcanology (plumes of degassed or primitive magma entering a turbulent magma chamber, volcanic gas plumes in turbulent atmospheres), ventilation studies (plumes of cool air moving through thermally convecting rooms) and environmental science (modelling sustained emissions from point sources, such as smoke or pollutants from chimney stacks, or sustained chemical leaks into a turbulent ocean).

Turner (1963) presented a theoretical model of a discrete release of buoyant fluid, or *thermal*, moving through a turbulent environment. He used a similar framework to Morton *et al.* (1956) but allowed for the removal of plume material by the turbulent environment, by making the dimensionally justified assumption that there exists an *extrainment* velocity, u_{out}, that is proportional to some characteristic velocity scale, V, within the environment. β is the *extrainment constant*, to be determined by experiment, where

$$u_{out} = \beta V. \tag{1.7}$$

In unstratified conditions, Turner's model predicts that entrainment is dominant near the source (where vertical velocities within the plume are greatest), so the thermal grows, and the density contrast between the thermal and its surroundings decreases. Further from the source entrainment becomes less important. The extrainment velocity remains constant, so extrainment becomes relatively more important. At a certain distance from the source, entrainment and extrainment balance and the thermal ceases to grow. At even greater distances, extrainment is dominant and the radius of the thermal decreases to zero, i.e. the thermal has been totally mixed into the environment. Note that Turner expressed doubt as to the applicability of the model in this 'shrinking' phase. Once the intensity of the turbulence within the plume has become equal to that in the environment (where $u_{in} = u_{out}$), he assumed that it can be regarded as part of the environmental turbulence, and speculated that the 'open parcel' model of Priestley (1953) may be more appropriate for this phase. Priestley (1953)

regarded the buoyant element as a region of constant size, which is interchanging fluid with its surroundings at a rate governed by the level of turbulence within the environment.

The behaviour of systems comprising both point-source plumes and the distributed buoyancy-flux characteristic of thermal convection was studied by Wells, Griffiths & Turner (1999). They found that if the plume buoyancy flux was greater than the distributed source, and acted in the opposite direction, asymptotic steady states can be established where convective mixing and plume stratification are balanced. This puts potential limits on the long-term behaviour of plumes in convecting environments, and we return to this concept in §5.

Netterville (1990) presented a time-dependent model of plume motion through a turbulent atmosphere based on observations of flow in free shear layers, accounting for the effect of wind as well as turbulence. However, a detailed knowledge of the environment is required, and the maximum plume rise height is undefined in the absence of wind. The theory developed in this study is complementary to that of Netterville (1990) in that, whilst it does not account for some of the detail of the latter, it gives a much simpler mechanistic view of the system, and can be applied when knowing only the convective velocity scale of the environment and plume source parameters.

A complete description of turbulent convection is not currently possible. However, much is known about the nature of turbulence and convection, and the relevant aspects are outlined here. For further reviews see Davidson (1957), Mathieu & Scott (2000) or Bejan (2004). The balance between conduction and convection of heat is described by the Rayleigh number, Ra, given by

$$Ra = \frac{ga\Delta T d^3}{\nu\kappa},\tag{1.8}$$

where a is the thermal expansion coefficient, ΔT is the temperature difference driving heat transfer, d is the thickness of the layer, ν is the kinematic viscosity and κ is the thermal diffusivity of the fluid. For $Ra > Ra_{crit}$, where Ra_{crit} is the critical Rayleigh number with a value of approximately 2000–3000 (Henke 1966), convection dominates the transfer of heat across the fluid. For $Ra > 10^6$, Deardorff & Willis (1967) found that convection is strongly time-dependent. This style of convection was termed *turbulent* by Huppert & Sparks (1984). The Reynolds number, Re, is defined as

$$Re = \frac{Vr}{\nu},\tag{1.9}$$

where V is the velocity scale and r is the radius of the flow. Turbulence is initiated when the Reynolds number exceeds some critical value (Re_{crit}), whose value depends on the flow configuration. Snyder (1981) found that the rise of buoyant plumes in calm, stratified conditions became turbulent when Reynolds numbers exceeded ∼200, though Hoult & Weil (1972) found that their theory for turbulent plume rise in a crossflow held for Reynolds numbers as low as 30. Measurement of Re in convection is difficult, so here we use the relationship of Grossmann & Lohse (2002), figure 1, to estimate Re from Ra and the Prandtl number, Pr, given by

$$Pr = \frac{\nu}{\kappa}.\tag{1.10}$$

Baines & Turner (1969) examined the mixing produced by a plume in a confined region with initially uniform density. Their model focused on the motion of the
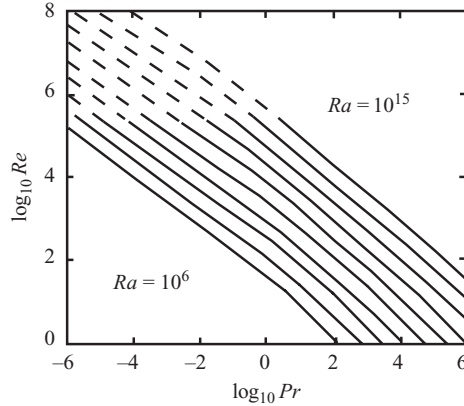
FIGURE 1. Relationship between Rayleigh number, *Ra*, Reynolds number, *Re*, and Prandtl number, *Pr*, after Grossmann & Lohse (2002).

so-called first front, which descends through the environment and across which there is an abrupt division between the original fluid in the environment and the fluid which has been cycled through the plume. They also showed how the density profile of the fluid behind this front could be determined by solution of the advection equation in the environment. This modelling was restricted to the idealized case of a pure source of buoyancy in which there is no source mass flux and in which there is only one opening. Linden, Lane-Serff & Smeed (1990) and subsequent workers extended the work to show that in a ventilated room with two openings, a steady regime becomes established with inflow through one opening and outflow through the other (e.g. Cooper & Linden 1996; Gladstone & Woods 2001). Worster & Huppert (1983) presented an approximate analytic expression for the time-dependent density profile for a plume in a confined region.

In the rest of this paper, we derive a theoretical model to describe sustained plume behaviour in a turbulently convecting environment, and compare model predictions with experimental observations. Note that, although plumes are also a form of convection, throughout the rest of this study we refer to convection exclusively in terms of the thermally driven convection. We consider a negatively buoyant sustained plume moving downwards through a turbulently convecting environment. Section 2 describes the derivation of a model, and §3 details the results of laboratory experiments to test it. In §4 we extend the model to account for the evolution of a finite environment, developing a 'filling-box' model, and show experimental justification for this model. A further discussion of the main findings of this study and examples of their utility in volcanology and ventilation studies are given in §5. Finally, in §6, we summarize our findings and conclusions.

2. Development of the theoretical model

2.1. *Derivation*

We follow the approach of Turner (1963) by assuming that fluid is 'extrained' from the plume by the turbulent environment at a velocity proportional to a characteristic velocity scale within the environment, V (equation 1.7). This assumption is analogous to the entrainment assumption of Morton *et al.* (1956), and is made on dimensional grounds. In order to be removed permanently from the plume, a parcel of fluid need

only be moved sideways a small distance, to a streamline of the mean motion that remains separate from the body of the plume. These streamlines can be near to the plume bounding surface for large proportions of that surface, so it is the short-range eddy-diffusion processes that are important to extrainment (Turner 1963). There is no evidence that any processes within the plume interior can affect this extrainment, so extrainment must be governed by properties of the environment (Turner 1963). The root-mean-square, or similar, turbulent-velocity scale is the natural choice upon which to scale the extrainment velocity. Note that in this description, the 'plume' is defined as being the region with overall motion governed by the plume source conditions. As fluid originating from the plume source is extrained to the environment, not all fluid that is originally part of the plume remains as part of the plume – a fundamental difference to plumes in static surroundings. The environment is assumed to be infinite, so that its density is unaffected by any exchange of fluid with the plume.

We define the volume (πQ), specific momentum (πM) and buoyancy (πF) fluxes as $\pi b^2 w$, $\pi b^2 w^2$ and $\pi b^2 w g'$, respectively, after Morton *et al.* (1956). Following their derivation we find three coupled ordinary differential equations describing the change in volume, momentum and buoyancy fluxes with distance from the source for the case with both entrainment and extrainment occurring

$$\frac{\mathrm{d}(b^2 w)}{\mathrm{d}z} = 2b(\alpha w - \beta V), \tag{2.1}$$

$$\frac{\mathrm{d}(b^2 w^2)}{\mathrm{d}z} = b^2 g' - 2bw\beta V, \tag{2.2}$$

$$\frac{\mathrm{d}(b^2 w g')}{\mathrm{d}z} = -b^2 w N(z)^2 - 2bg'\beta V. \tag{2.3}$$

These equations can be rearranged to give an equivalent set of equations in terms of b, w and g':

$$\frac{\mathrm{d}b}{\mathrm{d}z} = 2\alpha - \frac{bg'}{2w^2} - \frac{\beta V}{w}, \tag{2.4}$$

$$\frac{\mathrm{d}w}{\mathrm{d}z} = \frac{g'}{w} - \frac{2\alpha w}{b}, \tag{2.5}$$

$$\frac{\mathrm{d}g'}{\mathrm{d}z} = -N(z)^2 - \frac{2\alpha g'}{b}. \tag{2.6}$$

Note that these are identical to the governing equations of Morton *et al.* (1956) except for the addition of the $-\beta V/w$ term in (2.4). There is no general analytical solution for this system of equations, so they must be integrated for each set of initial conditions. As an example, we present the solutions that are applicable in the buoyancy-dominated case, i.e. when $Q_0 \sim M_0 \sim 0$ and F_0 is finite. In this case the only external parameters that can control the system are F_0 and V, as well as the entrainment and extrainment constants, α and β.

2.2. *Buoyancy-dominated plume model*

The parameters of the model system are non-dimensionalized such that

$$b = \frac{F_0 \alpha^2}{\beta^3 V^3} b_1, \tag{2.7}$$

$$z = \frac{F_0 \alpha}{\beta^3 V^3} z_1, \tag{2.8}$$

$$w = \frac{\beta V}{\alpha} w_1, \tag{2.9}$$

$$g' = \frac{\beta^5 V^5}{\alpha^3 F_0} g_1', \tag{2.10}$$

$$N = \frac{\beta^4 V^4}{\alpha^2 F_0} N_1, \tag{2.11}$$

where the subscript 1 indicates a dimensionless parameter. The dimensionless fluxes are related to these base parameters by $Q_1 = b_1^2 w_1$, $M_1 = b_1^2 w_1^2$ and $F_1 = b_1^2 w_1 g_1'$.

Substituting these dimensionless parameters into (2.4)–(2.6) gives three dimensionless differential equations that describe the buoyancy-dominated system

$$\frac{\mathrm{d}b_1}{\mathrm{d}z_1} = 2 - \frac{1}{w_1} - \frac{b_1 g_1'}{2w_1^2}, \tag{2.12}$$

$$\frac{\mathrm{d}w_1}{\mathrm{d}z_1} = \frac{g_1'}{w_1} - \frac{2w_1}{b_1}, \tag{2.13}$$

$$\frac{\mathrm{d}g_1'}{\mathrm{d}z_1} = -N_1^2 - \frac{2g_1'}{b_1}. \tag{2.14}$$

The solutions are singular at the origin. To generate appropriate starting conditions for the numerical integration, we balanced the dominant powers near the source to derive the following power series describing plume radius, velocity and reduced gravity as functions of z:

$$b_1 = \frac{6}{5} z_1 + \cdots, \tag{2.15}$$

$$w_1 = \left(\frac{25}{48}\right)^{1/3} z_1^{-\frac{1}{3}} + \cdots, \tag{2.16}$$

$$g_1' = \frac{4}{3} \left(\frac{25}{48}\right)^{2/3} z_1^{-5/3} + \cdots. \tag{2.17}$$

The integrations were initiated at depth $z_1 = 10^{-12}$ with corresponding values of: $b_1 = 1.2 \times 10^{-12}$, $w_1 = 8046$ and $g_1 = 8.6 \times 10^{19}$.

2.3. *Solution of equations*

The model of a buoyancy-dominated plume in turbulently convecting surroundings (equations (2.12)–(2.14)) was solved using the fourth order Runge Kutta procedure, 'rkf45', of the computer package Maple v9.5, with initial conditions as above (equations (2.15)–(2.17)). The relative tolerance, or maximum permitted relative discrepancy between the extrapolations from a given step length, and two steps of half that length, was 10^{-6}. Figure 2 shows the results of this integration. In the region near the source, entrainment dominates and the plume radius increases. Further from the plume source vertical velocity decreases, while the convective velocity remains constant, so extrainment begins to dominate over entrainment. The plume radius attains its maximum value of $b_1 = 0.025$ at $z_1 = 0.04$ and diminishes to zero at $z_1 = 0.06$. The solutions conform to expectation; a plume will penetrate far into a convecting environment if the plume velocities are significantly greater than those in the environment. In this case, the solution over a given length scale tends towards the 'no convection' case investigated by Morton *et al.* (1956). If the convective velocity scale is large compared with velocities in the plume, then the plume length is short:
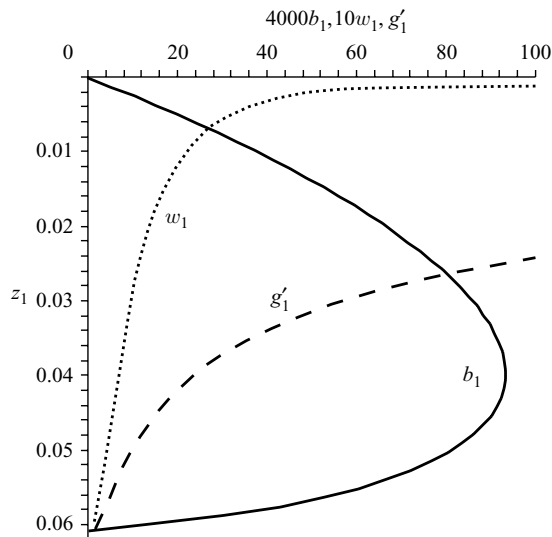
FIGURE 2. Dimensionless solutions for plume radius b_1 (solid), vertical velocity w_1 (dotted) and reduced gravity g'_1 (dashed) as a function of dimensionless depth below the plume origin z_1 for the buoyancy-dominated case, i.e. $Q_0 \sim M_0 \sim 0$. Scalings for these variables are given in (2.7)–(2.10).

the motion of the environment quickly dominates the effects of plume momentum and buoyancy. Any tracer sourced from the plume quickly becomes a passive tracer within the convecting environment. Note that these results are for the pure buoyancy plume. Hunt & Kaye (2001) have shown that any plume can be modelled as a pure plume with a virtual origin at a certain distance from the real source. If this distance is equivalent to dimensionless distance of $z_1 > 0.03$, then the plume may emerge from the source already in the extrainment-dominated phase. This is possible for plume sources with a momentum deficit – so-called 'lazy plumes'.

For comparison with experiment, and for the 'filling-box' models (§ 4.2) the equations were integrated using a similar fourth order Runge–Kutta scheme, programmed in C++ following the method of Press *et al.* (1986). A relative tolerance of 10^{-3} was used throughout.

2.4. *Richardson number dependence*

Recent work by Kaminski and coworkers (Kaminski, Tait & Carazzo 2005; Carazzo, Kaminski & Tait 2006) and Wang & Law (2002) has shown that α is not constant, but depends on the Richardson number. We assess the impact of this variation in figure 3. The parameterisation of α by Carazzo *et al.* (2006) is used to calculate model curves for a plume in turbulently convecting surroundings. Given the close agreement with the solutions found with a constant value of α we do not use these parameterizations further. The fine adjustments found by including such effects are of a secondary importance, in this scenario, to the extrainment process we study. Hunt & Kaye (2005) also found that a constant value of α fits data well, even for lazy or momentum-deficient plumes. Kaminski *et al.* (2005) noted that the α dependence is only normally manifested in compilations of data from experiments at different scales.
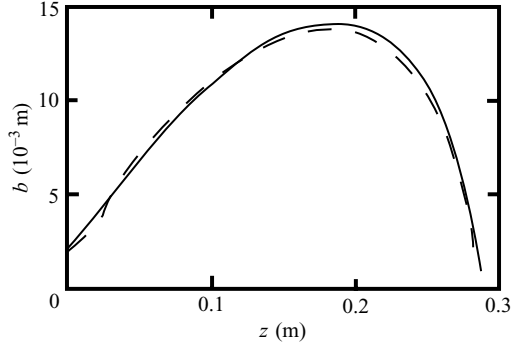
FIGURE 3. Modelled plume width as a function of depth assuming a constant entrainment factor, α, (solid) and a Richardson-number-dependent α (dashed) based on the parameterization of Carazzo *et al.* (2006).
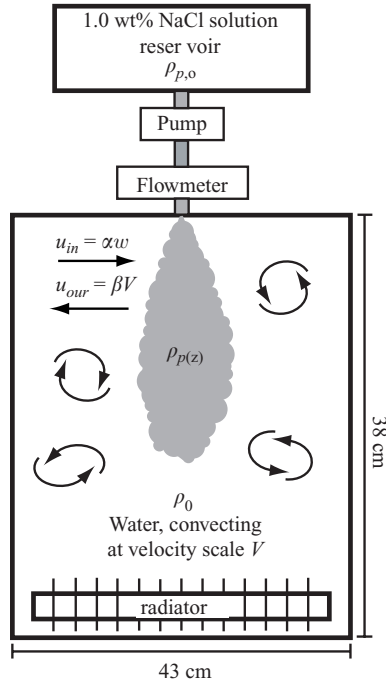

FIGURE 4. Experimental apparatus: the radiator causes turbulent thermal convection of the environment. The plume is visualized with a shadowgraph and dye.

3. Laboratory experiments

3.1. *Experimental apparatus and method*

The model derived in §2 was tested experimentally using the apparatus shown in figure 4. A tank of basal area $43\,\mathrm{cm} \times 39\,\mathrm{cm}$ and depth $38\,\mathrm{cm}$, filled with water, was heated by two radiators that covered the base of the tank. The heating drove turbulent convection within the tank with $Ra = 10^9$–10^{10} and $Re = 3000$–5000. Ra and Re were above their respective critical values for all experiments. The relationship of

Deardorff & Willis (1967),

$$V = 0.44 \left[\frac{(ga\Delta T)^4 \kappa^2 d^3}{\nu} \right]^{1/9}, \qquad (3.1)$$

valid for thermal convection at high Rayleigh numbers, was used to estimate convective velocity scales, and experimental observation of neutrally buoyant millimetre-scale particles within the tank verified that this relationship was valid to within experimental error for these experiments. In this expression $a = 4 \times 10^{-4}\,\mathrm{K}^{-1}$ is the thermal expansion coefficient, $\kappa = 1.4 \times 10^{-7}\,\mathrm{m}^2\,\mathrm{s}^{-1}$ is the thermal diffusivity, $d = 0.38\,\mathrm{m}$ is the vertical length scale and $\nu = 1 \times 10^6\,\mathrm{m}^2\,\mathrm{s}^{-1}$ is the kinematic viscosity. The convective velocity scale was varied, by a factor of 2, by altering the temperature difference, ΔT, between the radiators and the water within the tank. The accessible range of V was limited by the maximum temperature of hot water available for the radiators, and the form of the relationship between ΔT and V (equation (3.1)) – an ever increasing ΔT is required to drive a constant increase in V.

The convective velocity scale has a single value for given experimental conditions, although convective velocities observed within the tank were variable both spatially and temporally, with a standard deviation of 30 % of the estimated velocity scale. Therefore, any given (short time-scale) experiment may experience convective velocities that differ markedly from the estimated velocity scale, although we expect that the average of many experiments represents the long time-scale average behaviour of the system. In other words, whilst we predicted significant variability in any experimental data, we hoped to establish statistical limits to this variability, and make useful measurements of the average plume behaviour. The advantage of this experimental setup is that it recreates the variability present in a natural turbulently convective system.

3.2. *Plume source characteristics*

The nozzle design is similar to that of Dr Paul Cooper of the University of Wollongong, NSW, Australia, as described by Hunt & Linden (2001) and Phillips & Woods (2004). Tests of this source show that the zone of flow establishment ahead of the source is very small, <0.005 m. The entrainment factor for the source was measured using the 'filling-box' method of Baines & Turner (1969) to be 0.14 ± 0.04. Following Hunt & Linden (2001), the virtual origins for the source and flow conditions in these experiments were 1–2 cm behind the real source. The Reynolds number of the source was in excess of 100 for all experiments, and the plume appeared turbulent at the source. (Whilst above the minimum Re for which turbulent models are observed to hold (Hoult & Weil 1972), this is below the Re_{crit} found by Snyder 1981. Measurement of α with the lowest Re used in any experiment yielded a value of 0.18, implying that the entrainment is fully developed even at these low Reynolds numbers.)

In the infinite environment experiments (this section), plume liquid was dyed 1.0 wt % sodium chloride solution, with $0.0890\,\mathrm{m\,s^{-2}} < g_0' < 0.1273\,\mathrm{m\,s^{-2}}$, depending on the temperature difference between plume and ambient fluids. The experimental range of V was 0.00714–0.0138 m s^{-1}. The plume was visualized using a shadowgraph. Following the method of Turner (1963), the edge of the plume was identified using a combination of the edge of the region with turbulent eddies moving as a coherent plume and the edge of the dyed region. This approach helps to avoid the problem of dyed fluid no longer being part of the plume (§ 2.1). For each experiment between three and ten measurements of plume length at a particular instant were made by eye, with an estimated accuracy of ± 1 cm. The repeated measurements illustrate the natural variability of the system. The source volume, momentum and buoyancy fluxes

were varied by a factor 3; the minimum volume flux of $20\,\mathrm{cm^3\,s^{-1}}$ was the lowest that gave a turbulent plume from the source, and the maximum of $60\,\mathrm{cm^3\,s^{-1}}$ was the highest still giving a plume that was fully extrained within the confines of the tank.

3.3. *Results*

Conclusive experimental evidence for the process of extrainment by turbulent surroundings was found. Hydrochloric acid was added to the saline source and pH meters placed within $5\,\mathrm{mm}$ of the bounding surface of a plume with source $\mathrm{pH}=1.2$ moving through calm surroundings of $\mathrm{pH}=7.1$ did not detect any change in pH. This is in agreement with accepted plume theory, material is entrained into the turbulent plume from the surroundings, but no material leaves the plume. However, even with weak convection ($V/w_0=0.3$, where the subscript 0 indicates values at the plume source), the pH at $2\,\mathrm{cm}$ from the plume boundary rapidly dropped to below $\mathrm{pH}=6.3$, indicating that some acidified material from the plume interior was being removed into the environment. It was predicted that some form of diffusive profile would be found by measuring the pH as a function of radial distance from the plume. However, the data were very noisy, both spatially and temporally, because the length scale of thermal convection ($\sim5\,\mathrm{cm}$) is similar to the experimental length scale – acidic fluid is transported around the tank in highly variable patterns. Even time-averaged measurements showed no consistent pattern, as would be expected with such a naturally variable system. However, the important conclusion of these experiments is unchanged: fluid is removed from the plume in the presence of turbulent convection, but not in static surroundings. This observation has implications for measurement of the plume: a passive tracer sourced within the plume will not be retained exclusively within the plume. For example, a dyed plume will lose dyed fluid to the surroundings, so the boundaries of the dyed region will not correspond to the plume boundaries. To identify plume boundaries, some measurement of the plume motion must be made.

Figure 5 shows observations of the two end-member regimes of strong and weak plumes predicted in §2. Figure 5(*b*) shows a strong plume that reaches the base of the tank and forms a filling box, as in the study of Baines & Turner (1969). Figure 5(*a*) shows a weak plume, where all material is extrained to the surroundings before the plume reaches the base of the tank. Whilst highly variable, due to the short-time scale fluctuations in convective velocities and length scales, the 'end' of the plume (where $b\rightarrow0$) is the easiest and most robust measurement of plume behaviour to compare with model predictions. Figure 6 shows measurements of plume length compared to model predictions (with the best-fit values of entrainment and extrainment parameters $\alpha=\beta=0.1$). A line passing through the origin with a gradient of 1 forms the loci of data where the experiment corresponds exactly to the model predictions. This hypothetical line takes no account of the natural variability of the convective system, so one would not expect the observations to plot on such a straight line. The darkly and lightly shaded zones represent where data would plot if the average velocity experienced during a particular experiment were within 1 and 3 standard deviations, respectively, of the velocity scale (§3.1). The fact, that 86 % of the data plot inside the dark zone, and over 99 % of the data fall within the light zone, imply that the model provides a good description of the maximum length of a turbulent plume in turbulently convecting surroundings. If anything, we may have slightly overestimated the standard deviation of the velocity scale. While it makes intuitive sense that a weak plume in strong environmental turbulence will become fully incorporated into that turbulence, without a quantitative model, it would be difficult to predict over what length scale that incorporation would occur. Even an order of magnitude prediction for plume length
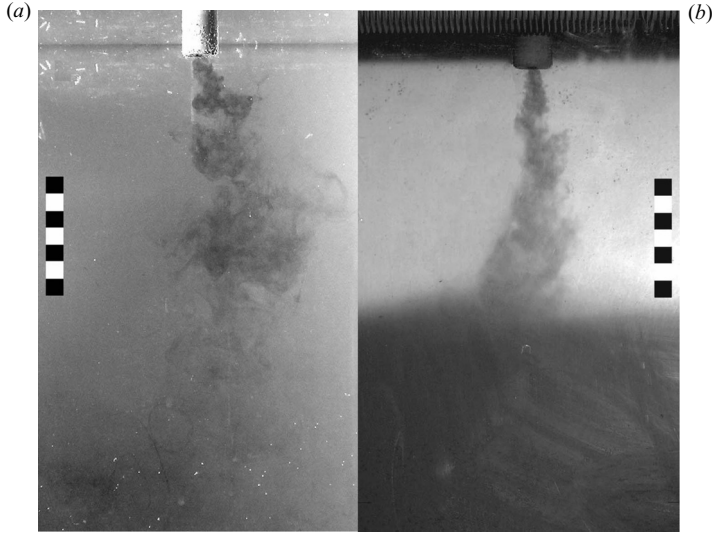
FIGURE 5. Photographs of plume end-member regimes. (*a*) A weak plume that is fully extrained to the surroundings, giving a well-mixed environment. Though $w_0 > V$, the rapid deceleration of fluid after leaving the source means $w \ll V$ over most of the plume. Experimental conditions: $b_0 = 0.002$ m, $w_0 = 0.05$ m s^{-1}, $g'_0 = 0.09$ m s^{-2}, $V = 0.015$ m s^{-1}. (*b*) A strong plume ($w \gg V$), giving rise to the 'convecting filling-box' regime modelled in §4. Experimental conditions: $b_0 = 0.002$ m, $w_0 = 0.4$ m s^{-1}, $g_0 = 2.0$ m s^{-2}, $V = 0.006$ m s^{-1} and $t = 150$ s. Scale bars have 1 cm squares.
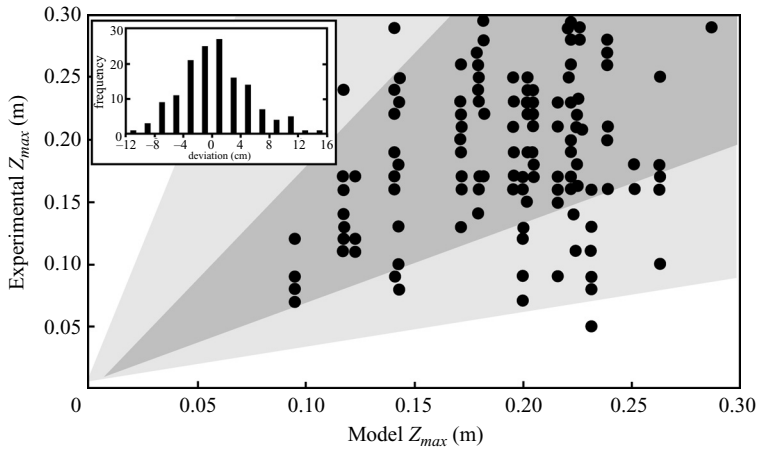

FIGURE 6. Plot of experimental data. The darkly and lightly shaded regions correspond to theoretical predictions for variations of the convective velocities of 1 and 3 standard deviations, respectively, from the mean V with $\alpha = \beta = 0.1$. The inset graph shows the frequency distribution of the deviation of the data from the 1:1 line. No data are obscured by the inset.

would be useful, and the experimental data indicate that the model is substantially more precise than that. The inset to figure 6 shows the frequency distribution of the offset of the data from the 1:1 line. The discrepancy is approximately normally distributed about zero offset, further supporting the suggestion that the scatter in the
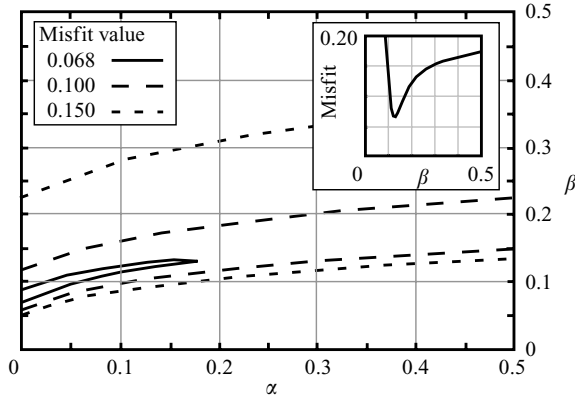
FIGURE 7. Contoured plot of misfit (M) as a function of entrainment (α) and extrainment (β) constants. The inset graph shows $M(\beta)$ for $\alpha = 0.14$ – the appropriate value for our plume source – indicating that $\beta = 0.13 \pm 0.02$ for these experimental conditions. The shallow gradient of the contours shows that this method of determining β is relatively insensitive to the value of α of the plume source.

data is caused by the natural variability of the system. These results also suggest that the model can predict the variability in plume lengths.

The optimum values for α and β were found as follows. A misfit function, M, was defined to quantify the discrepancy between experimental and modelled results, where x_e and x_m, respectively, are the experimentally measured and modelled values of the length of the plume;

$$M(\alpha, \beta) = \left[\frac{1}{n-1} \sum_{i=1}^{n} \left(x_{m_i} - x_{e_i} \right)^2 \right]^{1/2}. \tag{3.2}$$

The entrainment (α) and extrainment (β) factors were varied between 0.01 and 0.50, and the misfit calculated for each combination. The results of this analysis are given in figure 7 and show that the the method is relatively insensitive to α. Given the value of α determined in §3.2 ($\alpha = 0.14$), the best fit value for β is 0.13 ± 0.02. The inset to figure 7 shows the shape of the misfit minimum; β is very unlikely to be significantly less than 0.1, but could be somewhat more. For comparison, Turner (1963) found a value of β for thermals of 0.4, approximately double the value of α determined for thermals in static surroundings. In the case of thermals the environmental turbulence can extrain fluid from the leading and trailing boundaries. We speculate that this difference between thermals and plumes may account for the different values of β/α between this study and that of Turner (1963).

Figure 8(a) clearly demonstrates the increase in z_{max} as a function of Q_0. The z_{max} values are well within the range predicted for convective velocity variations of 1 standard deviation of V. The limited range of V accessible in the experiments precludes a rigorous, independent test of the dependence of z_{max} on V with all other variables fixed. Variations in V are included in the modelled results plotted in figure 6. For completeness we include figure 8(b), which shows that the reduction in z_{max} predicted by the theory for increasing V is observed, and is within the 1 standard deviation limit imposed by the temporal and spatial variability of convective velocities.

The nature of the decay of plume radius merits further discussion. Whereas the model predicts a smooth 'teardrop' shape to the end of the plume, this was not
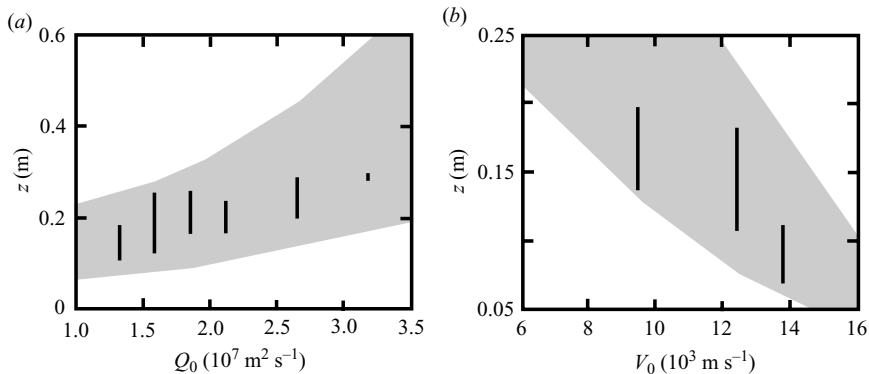
FIGURE 8. (*a*) $z_{max}(Q_0)$ for $V = 0.012 \, \mathrm{m \, s^{-1}}$; (*b*) $z_{max}(V)$ for $Q_0 = 1.3 \times 10^{-7} \, \mathrm{m^3 \, s^{-1}}$. Black bars represent the spread of experimental data. Dark regions show predictions for convective velocities within one standard deviation of V.

observed in the experiments. From the level of maximum plume width, the plume broke into individual eddies of (negatively) buoyant fluid that appeared to move independently, i.e. the plume did not behave as a coherent flow in its later stages. This effect was observed by Turner (1963) in thermals, and occurs because the turbulence within the plume becomes less intense than that in the environment. Turner's use of Priestley's (1953) model implies a 10% reduction in plume length will arise because of this effect. In view of the large natural variability of the observed system and the good agreement between the model and experiment, we have not included the effects described by Priestley (1953) here, thus keeping the model simple.

4. Plumes in a finite, convecting environment
4.1. *Derivation of model*

In many applications it is the evolution of an environment, rather than the plume, that is of interest. For example, the study of the evolution of turbulently convecting magma chambers, subject to the input of a turbulent plume of either fresh or degassed magma, is based on observations of the overall magma chamber composition rather than the plume (e.g. Huppert & Sparks, 1984). To this end, we extend our study by relaxing the assumption that the environment is infinite and unaffected by any exchange of material with the plume. We follow the approach of Baines & Turner (1969) by assuming a confined cylindrical environment of radius R and height H.

There are three density scales in this system, ρ_s is that of the environment, ρ_p is that of the plume and ρ_0 is a reference density, taken to be that of the environment at time $t = 0$. These lead to three reduced gravity scales:

$$g'_s = g \frac{\rho_s - \rho_0}{\rho_0}, \qquad (4.1)$$

$$g^*_p = g \frac{\rho_p - \rho_s}{\rho_s}, \qquad (4.2)$$

$$g'_{start} = g \frac{\rho_p - \rho_0}{\rho_0}, \qquad (4.3)$$

of which only g'_{start} is time-independent. (All terms, e.g. buoyancy fluxes, relating to the time-dependent density of the upper layer, ρ_s, are denoted by *.) If g'_s changes on
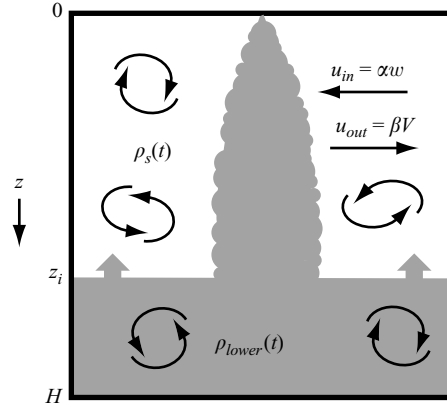
FIGURE 9. Schematic diagram of a plume in a finite convecting environment.

a longer time scale than that for a parcel of fluid in the plume to traverse the box, g'_s can be considered constant for any given instant for which the solutions of the plume model (§2) are found. It follows that the volume, momentum and buoyancy fluxes can be calculated at the level of the interface ($Q(z_i)$, $M(z_i)$, $F(z_i)$) for a given value of g'_s. There are two possible regimes. By conserving buoyancy in the system, solutions for both regimes can be derived. If the convection is sufficiently strong ($H > z_{max}$), the plume will not reach the base of the environment. In this end-member case, the convection within the environment will maintain a homogenous composition throughout the environment. The change in environmental density is given by

$$\frac{\mathrm{d} g'_s}{\mathrm{d} t} = \frac{F_0}{R^2 H}. \tag{4.4}$$

If, on the other hand, material from a (negatively) buoyant plume reaches the floor of the environment ($z_{max} > H$), it spreads horizontally as a gravity current. Once the lower layer is thick enough for spread to occur effectively instantly by pure shear within that layer, a 'filling-box' flow pattern is established, with a double-diffusive interface – stabilized by composition and destabilized by heat – separating two layers. We assume that the convection ensures that the upper layer is homogenous and that the compositional density difference between the upper and lower layers is sufficient to suppress convective mixing of the entire environment; this assumption is discussed further in section 4.3. The system is shown schematically in figure 9, and is analogous to that of Baines & Turner (1969). Note that the density stratification also inhibits the transfer of heat, and the convective velocities in the two layers will not be equal. The critical convective velocity is that in the layer in which the plume source is found (the upper layer in our system), and determines the convective velocity scale, V.

At all depths, the downwards flow within the plume is balanced by a net upwards flow within the environment of velocity U (Baines & Turner, 1969). We assume $R \gg b$ throughout, so that $U \ll w$, and the plume motion is unaffected by this upwards return flow. The interface between the two layers, at depth z_i, moves upwards (the opposite direction to plume motion) with time, t, at velocity U, where

$$U(z_i) = \frac{\mathrm{d} z_i}{\mathrm{d} t} = -\frac{Q(z_i)}{R^2}. \tag{4.5}$$

The amount of buoyancy extrained into the upper layer is given by the difference between the source buoyancy flux, F_0, and the buoyancy passing through the interface, $F(z_i)$, such that the change in reduced gravity of the upper layer is given by

$$\frac{\mathrm{d}g_s'}{\mathrm{d}t} = \frac{F_0 - F(z_i)}{R^2 z_i}. \tag{4.6}$$

As the density of the upper layer changes, the effective buoyancy and reduced gravity (g_p^*) of the plume are reduced such that

$$\frac{dF_0^*}{dt} = Q_0 \frac{dg_{p,0}^*}{dt}, \tag{4.7}$$

where the subscript 0 indicates values at the source $(z = 0)$ and

$$\frac{\mathrm{d}g_{p,0}^*}{\mathrm{d}t} = -\left(\frac{g_{start}'}{g} + 1\right)\left(1 + \frac{g_s'}{g}\right)^{-2} \frac{\mathrm{d}g_s'}{\mathrm{d}t}. \tag{4.8}$$

Equations (4.5)–(4.7) form a set of three coupled time-dependent ordinary differential equations that describe the evolution of the environment in the filling-box case. Note that the depth-dependent equations of §2 still need to be solved for each time step. Also notice that the buoyancy flux calculated directly by the plume model (equations (2.1)–(2.3)) is relative to the time-dependent reduced gravity g_p^*, whereas the reference buoyancy scale should be used. The buoyancy flux in the correct reference frame is given by

$$F(z_i) = \left[\left(\frac{g_p^*(z_i)}{g} + 1\right)\left(\frac{g_s'}{g} + 1\right) - 1\right] gb(z_i)^2 w(z_i). \tag{4.9}$$

The reduced gravity of the lower layer, g_{lower}', and hence its density, can be calculated by deducting the buoyancy of the upper layer from the total buoyancy emitted from the source, and dividing by the volume of the lower layer, giving

$$g_{lower}' = \frac{F_0 t - g_s' R^2 z_i}{(H - z_i)R^2}, \tag{4.10}$$

where all buoyancies are relative to the original reference density, ρ_0.

These equations were integrated using a fourth order Runge–Kutta scheme (Press *et al.* 1986) programmed in C++, with a relative tolerance of 10^{-2}. At each time step, the program calculates the motion of the interface, the density of the upper layer and therefore the buoyancy flux to be used in the next integration step. The plume equations (2.4)–(2.6) are also solved using the same Runge–Kutta scheme and relative tolerance.

4.2. *Solution of convecting filling-box model*

As with the plume model (§2), the equations must be integrated for each set of starting conditions. Here, we present the solutions for the case where the plume is controlled by the source buoyancy flux only. This allows us to use the dimensionless form of the plume model from §2.2. In addition to the dimensionless parameters contained therein, we must introduce dimensionless forms of R, H and t:

$$R = \frac{F_0 \alpha}{\beta^3 V^3} R_1, \tag{4.11}$$

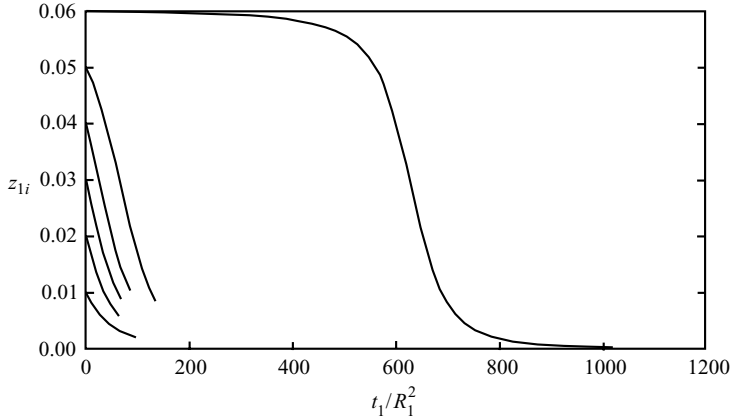$$H = \frac{F_0 \alpha}{\beta^3 V^3} H_1, \tag{4.12}$$

FIGURE 10. Modelled solutions for a buoyant plume in a finite convecting environment of dimensionless radius R_1 and various depths, H_1. Each solution starts with $z_{i,1}$, the dimensionless interface depth, equal to H_1 (left-hand axis) and ends when the densities of lower and upper layers are equal to within model resolution. This represents the latest time that single-layer convection will initiate, as thermal convection will penetrate the interface when the density contrast across it becomes sufficiently small.

$$t = \frac{F_0}{\beta^4 V^4} t_1. \tag{4.13}$$

The solutions were found by integrating the dimensional filling-box model (as described in §2.3) for parameter values within the buoyancy-dominated regime, then scaling the solutions as shown above. Note that (4.7) must be used after every time step to calculate the new lower value of effective source buoyancy flux. Various parameter values were used to ensure that the scaling was appropriate and collapsed the modelled data. The results of these integrations are shown in figure 10; initial conditions were: $b_0 = 0.004\,\mathrm{m}$, $w_0 = 1\,\mathrm{m\,s^{-1}}$, $g_{p,0}^* = 10^4\,\mathrm{m\,s^{-2}}$, $V = 0.01\,\mathrm{m\,s^{-1}}$, $R = 1.6 \times 10^7\,\mathrm{m}$, $\alpha = \beta = 0.1$. The time taken for given changes in density or interface depth to occur is proportional to the cross-sectional area of the box, so all results are presented as functions of t/R^2. No filling-box model is formed if $H_1 > 0.06$ as in this case the plume does not reach the floor of the environment, resulting in one homogenous layer. For $H_1 \to 0.06$, it is very unlikely that the density contrast between upper and lower layers will be sufficient to prevent convective mixing of the whole environment. All models show that the density contrast across the interface between the two layers decreases asymptotically towards zero. The integrations stop when the density contrast drops to within numerical resolution of zero, represented in figure 10 by the termination of the model curves. In the absence of a significant density contrast, thermal convection will cause mixing of the whole environment. Note that as the convection can overcome finite density contrasts, the terminations shown represent the latest time that the system will revert to single-layer convection. The $H_1 = 0.06$ curve takes a long time to fill because, at first, very little volume remains in the plume at the interface depth, causing the interface to move very slowly.

Most extrainment of buoyancy occurs near the source where the plume is very buoyant. Deep environments (large z_i) spread this buoyancy over a large volume so the rate of increase of buoyancy of the upper layer, compared to the lower layer, is slower than in shallow environments. This is reflected in the longer time taken for the deepest environments to mix convectively. These results have significant implications

for a variety of fields and applications. For example, a plume of buoyant magma entering a slowly convecting magma chamber would initially cause a zoned chamber to develop. Eventually, the densities of the two layers would become similar, and the whole chamber would overturn, possibly with significant consequences such as the onset of a new phase of volcanic activity.

4.3. *Experimental investigation*

In order to ensure that the convection was vigorous within the layer containing the plume source, the orientation of the 'filling-box' experiments was inverted with respect to that in §3. The plume source was therefore at the same boundary as the radiator. Positively buoyant dyed methanol was used as the plume liquid. For consistency with the previous analysis, we hereon describe the system as a downward-moving negatively buoyant plume; figure 5(*b*) has been inverted accordingly.

With low convective velocities ($< 0.006\,\mathrm{m\,s^{-1}}$), a two-layer system was indeed established (figure 5*b*). For large convective velocities ($V > 0.01\,\mathrm{m\,s^{-1}}$), the density contrast between the layers was overcome by thermal convective plumes, and the whole environment was mixed uniformly (figure 5*a*). We predicted that convective mixing of the entire environment would occur when the thermally induced density difference of the convective plumes exceeds the density difference between the two layers. However, even if thermal plumes cannot penetrate through the interface, convective 'erosion' of one layer by the other may occur. We assess the importance of convective mixing here, though the details are beyond the scope of this work; detailed studies are provided by Cardoso & Woods (1996), Jellinek, Kerr & Griffiths (1999) and Strang & Fernando (2001).

It follows that there are two complementary processes occurring in the convecting filling box: the extrainment described in this work (which is the effect we are trying to measure), and the turbulent mixing across the density interface (Cardoso & Woods 1996; Strang & Fernando 2001). Both cause the box to fill more slowly than the no-convection case modelled by Baines & Turner (1969). We used the model of Cardoso & Woods (1996) to assess the rate of mixing. They found that the speed of the interface is given by

$$\frac{\mathrm{d}z_i}{\mathrm{d}t} = \frac{Vc}{Ri} \tag{4.14}$$

where c is a constant between 0.1 and 0.3 (Zilitinkevich 1991) and Ri is the Richardson number, given by Cardoso & Woods (1996) as

$$Ri = \frac{g_p^* z_i}{V^2}. \tag{4.15}$$

$Ri = 60$ in these experiments, giving $\mathrm{d}z_i/\mathrm{d}t = 3 - 9 \times 10^{-5}\,\mathrm{m\,s^{-1}}$ (Cardoso & Woods 1996). We measured the extent of convective mixing by establishing a filling box and observing the motion of the interface in the presence of turbulent convection but absence of a plume. This method gave values of $\mathrm{d}z_i/\mathrm{d}t = (1.6 \pm 0.9) \times 10^{-4}\,\mathrm{m\,s^{-1}}$, in broad agreement with, though up to a factor of 2 greater than, the values predicted by Cardoso & Woods (1996).

Quantitative experiments to investigate the rate of motion of the density interface were carried out. The source, releasing positively buoyant methanol, was placed at the base of the tank with the radiators so as to ensure that the plume moved through a convecting layer. A 'filling box' was established under static ambient conditions, with the interface at $z_i \sim 0.25\,\mathrm{m}$. (Convection postponed the initial establishment of the density interface, reducing the times that experiments could be run for. Once
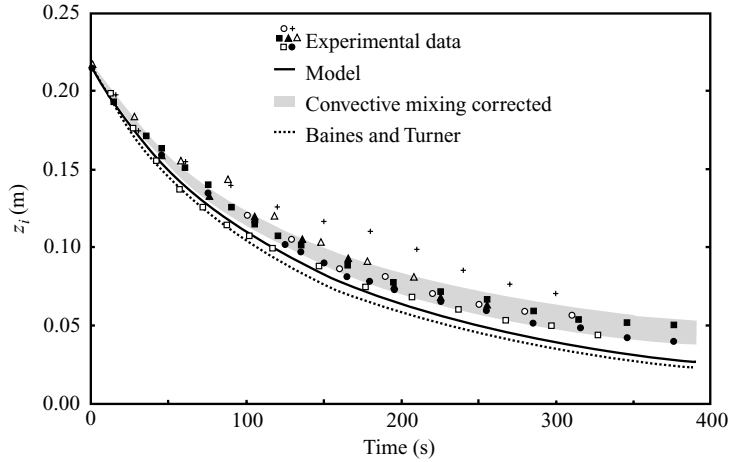
FIGURE 11. Comparison between experiment and modelled predictions for the motion of the interface of the convecting filling-box model. Conditions are $b_0 = 0.002$ m, $w_0 = 0.4$ m s^{-1}, $g'_0 = 2.0$ m s^{-2}, $V = 0.006$ m s^{-1}. The different symbols show results from repeated experiments at the same conditions. The shaded region shows the variation in convective mixing predicted by Cardoso & Woods (1996). The combination of convective mixing and extrainment account for these data well.

established, the density interface became an effective barrier to convective mixing.) Figure 11 shows experimental and modelled results for the motion of the density interface. Results for the no-convection (Baines & Turner 1969), convection-driven extrainment (this study), and extrainment plus mixing (Cardoso & Woods 1996) models are shown. The combination of extrainment and convective mixing (shaded region) accounts for the data well. Observations plotting above the shaded region were obtained in experiments where the convective mixing rate, measured subsequently, was particularly high (2.7×10^4 m s^{-1}). The temperature difference driving convection was maintained to within $2\,^\circ$C, but, as noted in §3.1, convective velocities vary with a standard deviation of $\sim 30\,\%$ of the mean value, which probably accounts for the variability in convective mixing rate. Figure 11 shows that both experiments and predictions tend towards a steady state, in agreement with the predictions for the long-term steady state of adjacent point and distributed buoyancy sources of Wells *et al.* (1999). The interface eventually ceased to be sharp and broadened into a mixing zone, also in agreement with Wells *et al.* (1999). We interpret this to be the beginning of convective mixing of the whole environment, as predicted at long time scales for the buoyancy-dominated case modelled in §4.2. We note that convective mixing causes the majority of the deviation from the no-convection case, and these experimental data are therefore not a rigorous validation of the extrainment model. There does not seem to be away to avoid this ambiguity as the two effects have a common cause. Given that we have shown the existence of extrainment (section 3), we simply assert that despite being equivocal, our extrainment model is consistent with these experimental data.

The volume extrainment rate in our model is proportional to the surface area of the plume in the upper layer, which scales as H^2. The cross-interfacial mixing rate is proportional to the cross-sectional area of the box, $A = (H/I)^2$ (where I is the aspect ratio of the box), and inversely proportional to Ri (Cardoso & Woods 1996). Ri is proportional to the reduced gravity difference across the interface (equation 4.15),

but given the homogenization of the fluids on each side of the interface, this reduced gravity is approximated well by the initial value of plume reduced gravity at the base of the box, $g_p^*(H)$, which, for pure plumes, scales as $H^{-5/3}$ (Morton *et al.* 1956). It follows that the interfacial mixing rate is proportional to $H^{8/3}$, i.e. as the length scales become larger, interfacial mixing dominates over volume extrainment. Volume extrainment is proportional to V, whereas interfacial mixing scales as V^3, so larger velocities also favour the latter mechanism. The significance of volume extrainment is therefore accentuated by very shallow environments, i.e. smaller than the scale of our experiments. We therefore expect mixing across the interface to dominate over the extrainment of volume from the plume in most situations. Note that very tall thin boxes do promote the effect of extrainment compared to cross-interfacial mixing, but such high-aspect-ratio cases invalidate the assumption of $R \gg b$ (§ 4.1).

The situation is different when considering the extrainment of a tracer from a plume and its resultant concentration in the environment. Cross-interfacial mixing of a tracer scales with both the cross-interfacial volume mixing rate and tracer concentration in the lower layer, i.e. on $H^{8/3} H^{-5/3} = H$. Note that mixing in the lower layer means that both Ri and tracer concentration do not change significantly as the box fills, so cross-interfacial mixing scales on the total box depth, H, rather than upper layer depth z_i. Assuming a top-hat tracer concentration within the plume, tracer extrainment per unit depth scales as $H^{-2/3}$ and is thus dominated by extrainment near to the source where the tracer is relatively concentrated. Hence, the total tracer extrainment rate into the upper layer remains effectively constant. In many situations, this near source extrainment dominates over any cross-interfacial mixing of the tracer, especially when the upper layer is shallow. This near-source extrainment is illustrated by the acidic tracer experiments described in § 3.3. Extrainment is therefore an important effect to consider when simulating, for example, hazardous chemical concentrations sourced from a plume in a finite environment. In cases such as this, even small tracer concentrations can have a large impact.

5. Discussion and applications

Whilst we have discussed observations and results throughout this study, it is appropriate to discuss some aspects more fully. The basis of the model and major predictions is robust. Our derivation is entirely consistent with that of Turner (1963) for thermals in a turbulent environment. The fundamental assumption that extrainment occurs when in turbulent surroundings is unequivocally observed in experiments (§ 3.3). At first glance, the correlation between results and model predictions might seem poor. However, there are good reasons for the range of results obtained, of which experimental error forms only a small fraction. Convecting systems are both temporally and spatially highly variable. Preliminary experiments showed that both large-scale circulation and relatively homogenous convection could arise from experimental conditions that were, as near as possible, identical. (Homogenous conditions were often unstable to a circulatory state.) Even with the near-homogenous convection that we were studying, occasional particularly strong thermal plumes and eddies could cause significant changes to observed plume behaviour. These events were not isolated, but merely the extremes of a continuum of length and velocity scales that characterizes the experimental and, presumably, natural conditions. With this in mind, it is naïve to think that the behaviour of a plume in such a variable environment will be steady and consistent, despite constant source conditions. The application of more sophisticated experimental techniques, such as particle velocimetry, would not address

these issues, and we therefore do not believe they would improve the reliability of the results.

Despite this variablility, the agreement between experiment and theory is good. Without any physical model, it would be impossible to make rigorous estimates of the length, radius and density of a plume surrounded by significant turbulence. The simplest approach would be dimensional analysis, leading to a length scale based on the buoyancy flux and a convective velocity scale. This is how we have scaled our results, and we have shown that the appropriate coefficient for this length scale is 0.06. Any estimates based on dimensional analysis alone would be inaccurate by almost a factor of 20. Order of magnitude estimates are very useful in a variety of fields, and our results suggest that the model presented here is at least precise enough to provide these.

In the 'convecting filling-box' model (section 4) it is assumed that both layers remain homogenous at all times. The convective velocity scale, V, for all experiments was of order $1 \, \mathrm{cm \, s^{-1}}$, whereas the speed of the interface was of order $0.05 \, \mathrm{cm \, s^{-1}}$, suggesting that convection would indeed thoroughly mix each layer on a much shorter time scale than that over which fluid was added to the layer. Visual observations also indicated that both layers were homogenous at all times during the experiments. The competition between the tendencies of the plume to stratify the environment and the convection to mix it leads to an interesting spectrum of behaviour. Wells *et al.* (1999) found that a steady, stratified state can be established if the plume buoyancy flux is significantly greater than the thermal buoyancy flux of convection. We have shown that extrainment from the plume will continuously reduce the effective plume buoyancy flux, so that convective mixing will eventually dominate the system. The density of the upper layer is strongly affected by extrainment, especially when its depth is small.

We now present two examples of the application of this model. Persistently degassing volcanoes, e.g. Masaya Volcano, Nicaragua, are observed to emit large quantities of gas despite negligible lava output. In order to maintain this gas flux, magma must ascend to near the surface, degas and return to a large subterranean reservoir. Active basaltic magma chambers convect vigorously (Huppert & Sparks 1984), and can be modelled as a turbulently convecting reservoir. The degassed magma is denser than volatile-rich magma ($g' = 0.06 \, \mathrm{m \, s^{-2}}$, Richet *et al.* 2000), and will therefore form a negatively buoyant plume within the convecting environment. If the dimensionless depth of the reservoir (H_1) is less than 0.03, the plume will reach the base of the reservoir with a substantial density contrast, and so establish a 'filling-box' flow pattern. The zonation of volatiles within the reservoir can have significant effects on the evolution of the reservoir, and affect the likelihood of eruption. Given a reservoir of $H = 100 \, \mathrm{m}$ and a mass flux ($\pi b^2 w$) of $9 \, \mathrm{m^3 \, s^{-1}}$ (estimated for Masaya Volcano by Stoiber, Williams & Huebert 1986), it follows from the dimensionless solutions of §2.2 that a 'filling box' will be established if the convective velocity is less than $0.2 \, \mathrm{m \, s^{-1}}$.

With regard to ventilation, consider an auditorium, 5 m high, with an audience who maintain a thermal boundary layer at the base 10 °C warmer than ambient. Given the following air properties (Weast 1967): $\kappa = 2.1 \times 10^{-5} \, \mathrm{m^2 \, s^{-1}}$; $a = 3.7 \times 10^{-3} \, \mathrm{K^{-1}}$; $\nu = 1.5 \times 10^{-5} \, \mathrm{m^2 \, s^{-1}}$; the Rayleigh and Reynolds numbers are estimated as $Ra \sim 10^{11}$ and $Re \sim 10^{4}$ (Grossmann & Lohse 2002), implying turbulent convection. The relationship of Deardorff & Willis (1967, equation 3.1) gives a convective velocity scale of $0.14 \, \mathrm{m \, s^{-1}}$. A ventilation system situated on the ceiling supplies cool air to the auditorium, which falls as a negatively buoyant plume through the convecting surroundings. Again using the buoyancy-dominated dimensionless solutions (section 2.2),

if $H_1 = H\beta^3 V^3 / F_0 \alpha < 0.03$, the plume will reach the audience with a significant temperature contrast; if $H_1 > 0.06$ the plume will be uniformly mixed into the surroundings before reaching the audience. To achieve the former scenario, a buoyancy flux of $F_0 > 5 \times 10^{-3} \, \mathrm{m^4 \, s^{-3}}$ must be supplied at the ventilation source. Given an air density of $1.2 \, \mathrm{kg \, m^{-3}}$ and specific heat capacity of $1010 \, \mathrm{J \, kg^{-1} \, K^{-1}}$ (Weast 1967), this translates to a cooling system rated at $150 \, \mathrm{W}$.

6. Conclusions

We have presented a theoretical description of the behaviour of plumes in turbulently convecting environments. The model is based on that of Morton *et al.* (1956), but assumes that the turbulent environment *extrains* fluid from the plume as well as the plume entraining material from the environment. On dimensional grounds we assume that the extrainment velocity is proportional to a characteristic velocity scale within the environment, with an extrainment constant, β. We predict that, near a pure buoyancy source, plumes grow as they entrain fluid from the surroundings. Further from the source, plume velocities decrease and extrainment becomes dominant over entrainment. The rate of plume growth with height decreases to zero, then the plume radius rapidly diminishes to zero. Lazy plumes (with a momentum deficit, cf. a pure buoyancy plume) may be dominated by extrainment from the source.

Our model agrees well with experimental observations. We have shown conclusively that fluid is extrained from a plume by a turbulent environment, in agreement with a similar study of thermals (Turner 1963). The lengths of plumes with various source fluxes and environmental convective velocity scales have been predicted. Comparison with experiment yielded an extrainment constant of $\beta \sim 0.1$, similar to the entrainment constant. A major feature of the experiments is that the actual convective velocities experienced by any particular packet of plume material can vary widely from the spatially and temporally averaged velocity scale, with an estimated standard deviation of 30% of the mean velocity. Consequently, the maximum plume length varies through time. This aspect of the experiments is a natural consequence of any high Rayleigh number convection, and is to be expected in natural situations. The fact that the model can predict both the long-term average, and to a certain extent the variability of plume length, suggests that it is applicable in these highly variable settings.

A description of plumes in a finite convecting environment has also been derived. The end-member predictions of the model (homogenous environment at high convective velocities; 'filling-box' model, analogous to that of Baines & Turner 1969, at low convective velocities) are observed in experiments. The effect of volume extrainment is minor compared to convective mixing across the density interface, but can have a large impact on the environmental concentration of tracers sourced from the plume. When convective mixing across the filling-box density interface is also accounted for, the model describes experimentally observed behaviour well. Importantly, it was predicted that while a buoyancy-dominated plume would initiate a 'filling box' if convection is sufficiently slow, the density contrast between the two layers would gradually diminish to the point that thermal convection can overcome the density stratification. At this point the environment would rapidly become well mixed.

REFERENCES

BAINES, W. D. & TURNER, J. S. 1969 Turbulent convection from a source in a confined region. *J. Fluid Mech.* **37**, 51–80.

BEJAN, A. 2004 *Convection Heat Transfer*, 3rd edn. Wiley.

CARAZZO, G., KAMINSKI, E. & TAIT, S. 2006 The route to self-similarity in turbulent jets and plumes. *J. Fluid Mech.* **547**, 137–148.

CARDOSO, S. S. S. & WOODS, A. W. 1996 Interfacial turbulent mixing in stratified magma reservoirs. *J. Volcanol. Geotherm. Res.* **73**, 157–175.

COOPER, P. & LINDEN, P. F. 1996 Natural ventilation of an enclosure containing two buoyancy sources. *J. Fluid Mech.* **311**, 153–176.

DAVIDSON, P. A. 1957 *Turbulence: An Introduction for Scientists and Engineers*. Oxford University Press.

DEARDORFF, J. W. & WILLIS, G. 1967 Investigation of turbulent thermal convection between horizontal plates. *J. Fluid Mech.* **28**, 675–704.

GLADSTONE, C. & WOODS, A. W. 2001 On buoyancy-driven natural ventilation of a room with a heated floor. *J. Fluid Mech.* **441**, 293–314.

GROSSMANN, S. & LOHSE, D. 2002 Prandtl and rayleigh number dependence of the reynolds number in turbulent thermal convection. *Phys. Rev.* E **66**, 016305.

HENKE, R. W. 1966 *Introduction to Fluid Mechanics*. Addison-Wesley.

HOULT, D. P. & WEIL, J. C. 1972 Turbulent plume in a laminar cross flow. *Atmos. Environ.* **6**, 513–531.

HUNT, G. R. & KAYE, N. G. 2001 Virtual origin correction for lazy turbulent plumes. *J. Fluid Mech.* **435**, 377–396.

HUNT, G. R. & KAYE, N. G. 2005 Lazy plumes. *J. Fluid Mech.* **533**, 329–338.

HUNT, G. R. & LINDEN, P. F. 2001 Steady-state flows in an enclosure ventilated by buoyancy forces assisted by wind. *J. Fluid Mech.* **426**, 355–386.

HUPPERT, H. E. & SPARKS, R. S. J. 1984 Double diffusive convection. *Annu. Rev. Earth and Planet. Sci.* **12**, 11–37.

JELLINEK, A. M. & KERR, R. C. 1999 Mixing and compositional stratification produced by natural convection 2. applications to the differentiation of basaltic and silicic magma chambers and komatiite lava flows. *J. Geophys. Res.* **104** (B4), 7203–7218.

JELLINEK, A. M., KERR, R. C. & GRIFFITHS, R. W. 1999 Mixing and compositional stratification produced by natural convection 1. Experiments and their application to earth's core and mantle. *J. Geophys. Res.* **104** (B4), 7183–7201.

KAMINSKI, E., TAIT, S. & CARAZZO, G. 2005 Turbulent entrainment in jets with arbitrary buoyancy. *J. Fluid Mech.* **526**, 361–376.

LEE, J. H. W. & CHU, V. H. 2003 *Turbulent Jets and Plumes – A Lagrangian Approach*. Kluwer.

LINDEN, P. F., LANE-SERFF, G. F. & SMEED, D. A. 1990 Emptying filling boxes: the fluid mechanics of natural ventilation. *J. Fluid Mech.* **212**, 309–335.

LIST, E.J. 1982 Turbulent jets and plumes. *Annu. Rev. Fluid Mech.* **14**, 189–212.

MATHIEU, J. & SCOTT, J. 2000 *An Introduction to Turbulent Flow*. Cambridge University Press.

MORTON, B. R., TAYLOR, G. I. & TURNER, J. S. 1956 Turbulent gravitational convection from maintained and instantaneous sources. *Proc. R. Soc. Lond.* A **234**, 1–23.

NETTERVILLE, D. D. 1990 Plume rise, entrainment and dispersion in turbulent winds. *Atmos. Environ.* **24A**, 1061–1081.

PHILLIPS, J. C. & WOODS, A. W. 2004 On ventilation of a heated room through a single doorway. *Building & Environ.* **39**, 241–253.

PRESS, W. H., FLANNERY, B. P., TEUKOLSKY, S. A. & VETTERLING, W. T. 1986 *Numerical Recipies in Pascal*, 1st edn., *Numerical Recipies*, vol. 1. Cambridge University Press.

PRIESTLEY, C. H. B. 1953 Buoyant motion in a turbulent environment. *Austral. J. Phys.* **6**, 279–290.

RAJARATNAM, N. 1976 *Turbulent Jets*. Elsevier.

RICHET, P., WHITTINGTON, A., HOLTZ, F., BEHRENS, H., OHLHORST, S. & WILKE, M. 2000 Water and the density of silicate glasses. *Contrib. Mineral. Petrol.* **138**, 337–347.

SNYDER, W. H. 1981 Guideline for fluid modelling of atmospheric diffusion. *Tech. Rep.* US Environment Protection Agency.

STOIBER, R. E., WILLIAMS, S. N. & HUEBERT, B. J. 1986 Sulfur and halogen gases at Masaya caldera complex, Nicaragua: total flux and variations with time. *J. Geophys. Res.* **91** (B12), 12215–12231.

STRANG, E. J. & FERNANDO, H. J. S. 2001 Entrainment and mixing in stratified shear flows. *J. Fluid Mech.* **428**, 349–386.

TURNER, J. S. 1963 The motion of buoyant elements in turbulent surroundings. *J. Fluid Mech.* **16**, 1–16.

TURNER, J. S. 1979 *Buoyancy Effects in Fluids*. Cambridge University Press.

WANG, H. & LAW, A. W.-K. 2002 Second-order integral model for a round turbulent buoyant jet. *J. Fluid Mech.* **459**, 397–428.

WEAST, R. C. 1967 *Handbook of Chemistry and Physics*, 48th edn. Cleveland: Chemical Rubber Company.

WELLS, M. G., GRIFFITHS, R. W. & TURNER, J. S. 1999 Competition between distributed and localized buoyancy fluxes in a confined volume. *J. Fluid Mech.* **391**, 319–336.

WORSTER, M. G. & HUPPERT, H. E. 1983 Time-dependent density profiles in a filling box. *J. Fluid Mech.* **132**, 457–466.

ZILITINKEVICH, S. S. 1991 *Turbulent Penetrative Convection*. Avebury.